RESEARCH ARTICLE

Intracellular Water Dynamic Traits in Detached Leaves of Two Brassicaceae Plant Species under Saturated and Non-saturated Water Conditions

Yuxuan Gong[1], Deke Xing[1,*], Linpu Wu[1], Huiwen Chen[1], Junle Li[1] and Qian Zhang[1]

[1] School of Agricultural Engineering, Jiangsu University, Zhenjiang 212013, China

Abstract

Investigating the intracellular water dynamics within leaves will clarify plant responses to different water conditions and provide a theoretical basis for enhancing water-use efficiency. Detached leaves of Chinese flowering cabbage (*Brassica campestris* L. ssp. *chinensis* var. *utilis* Tsen et Lee) and broccoli (*Brassica oleracea* L. var. *italica* Plenck) were used as experimental materials in this study. Electrophysiological parameters of the leaves under saturated and non-saturated conditions were measured, and the intracellular water, nutrient, and energy related indices were calculated according to Nernst equation. The acceleration (a) reflecting the change rate of water transport rate in cells was defined and calculated, and the response characteristics of the two plant species to water were analyzed. The results showed that leaf intracellular metabolic activities of the two plant species were better in the saturated condition than those in non-saturated condition, and electrophysiological parameters could reflect the intrinsic characteristics and potential of the plants. Under saturated water condition, the intracellular water transport rate, electrophysiological ion transport efficiency and low nutrient tolerance of *B. campestris* were significantly higher than those of *B. oleracea*, and *B. campestris* showed high cell metabolic energy and metabolic activity. From non-saturated to saturated condition, the intracellular water transport rate of *B. campestris* changed rapidly, but the increase rate of intracellular water holding capacity was low, while that of *B. oleracea* was just the opposite. Therefore, *B. campestris* exhibited higher water sensitivity compared to *B. oleracea*.

Keywords: intracellular water, electrophysiological ion transport efficiency, cell metabolic energy, cell metabolic activity, acceleration.

1 Introduction

Brassicaceae family boasts remarkable species diversity, with its members delivering critical benefits including food security, aesthetic value, medicinal resources, and other economic contributions. Chinese flowering cabbage (*Brassica campestris* L. ssp. *chinensis* var. *utilis* Tsen et Lee) is an annual or biennial herb of the genus Brassica (Brassicaceae). Derived from the pak-choi complex via centuries of intensive artificial selection and domestication, this southern China-native specialty vegetable is valued for its high

Submitted: 09 December 2025
Accepted: 27 March 2026
Published: 30 March 2026

Vol. 1, **No.** 1, 2026.
10.62762/JPE.2025.989558

***Corresponding author:**
✉ Deke Xing
xingdeke@ujs.edu.cn

Citation
Gong, Y., Xing, D., Wu, L., Chen, H., Li, J., & Zhang, Q. (2026). Intracellular Water Dynamic Traits in Detached Leaves of Two Brassicaceae Plant Species under Saturated and Non-saturated Water Conditions. *Journal of Plant Electrobiology*, 1(1), 42–57.

nutritional content and tender texture, serving as both a popular culinary ingredient and a traditional medicinal resource. It is now widely consumed in South China, supported by large-scale cultivation and substantial annual yields [1]. Broccoli (*Brassica oleracea* L. var. *italica Plenck*), another annual or biennial Brassica species (Brassicaceae), originated in Italy and was later introduced to southern China, evolving into a globally cultivated crop. Its edible parts include crisp-tender floral stalks, shortened succulent peduncles, and tightly clustered florets. Renowned for its rich nutrient profile, particularly high protein content in stems and leaves, *B. oleracea* is highly favored by consumers. As the world's largest vegetable exporter and a top global producer, China plays a pivotal role in the global *B. oleracea* supply chain [2]. Despite the continuous expansion of China's vegetable export trade, it faces growing challenges that necessitate improved production efficiency and quality to maintain international competitiveness. Among key agronomic practices, water management is critical for determining yield and produce quality. Investigating the intracellular water dynamics of *B. campestris* and *B. oleracea* will clarify their species-specific responses to water conditions, ultimately providing a theoretical basis for enhancing vegetable quality and water-use efficiency.

All vital plant processes are inseparable from water, which participates in photosynthesis, respiration, and the synthesis and degradation of organic compounds, thereby exerting profound impacts on plant growth, physiology, and biochemistry [3–5]. Exposure to water stress often induces water imbalance in plants, disrupting developmental programs and yield formation; in severe cases, it even threatens survival [6, 7]. While plants can re-establish tissue water balance through intrinsic transport regulation to maintain normal growth, this adaptive capacity is species-specific, resulting in distinct water-use patterns across crop species [8]. Leaves, as the primary sites of photosynthesis and transpiration, are the plant organs most sensitive to environmental changes. Functionally, they act as a "safety valve" in the plant's water transport system: during water movement within leaves, water can be temporarily retained, and its release into the transpiration stream regulated. This mechanism reduces water loss, maintains internal water balance, and sustains photosynthesis and growth [9]. Approximately 97% of water absorbed by roots is lost via transpiration, with only 1–3% retained for metabolic processes. Photosynthesis is sensitive to such water dynamics, yet its response to leaf water content is rarely a simple linear relationship [10]. This non-linearity arises from the 1–3% of water sequestered in leaf cells. As stress intensifies, this sequestered water becomes increasingly critical, disproportionately governing whole-plant water status.

Under varying water conditions, the morphological structure and hydraulic properties of plant leaves undergo modifications that subsequently regulate intracellular metabolic processes and alter plant water and EITE (electrophysiological ion transport efficiency). Drought stress significantly reduces the thickness of palisade and spongy tissues as well as vein diameter of Betula pendula, accompanied by a marked increase in osmolyte accumulation [11]. In cotton, rapid stomatal closure restricts CO_2 diffusion, leading to immediate inhibition of carbon assimilation [12]. Similarly, flooding stress decreases stomatal conductance and transpiration rate in Rhododendron leaves [13, 14]. Water transport in plant tissues (including leaves) is driven by transpirational pull, which also plays a critical role in nutrient translocation and distribution throughout the plant [15]. Drought treatment enhances the uptake, accumulation, and distribution of specific mineral elements in Cunninghamia lanceolata leaves [16]. Conversely, increased water availability promotes the mass flow of dissolved nutrients to root surfaces and their subsequent delivery to leaves via the xylem [17]. Tomato maintains vigorous leaf metabolic activity, strong photosynthetic and transpirational fluxes, and efficient nutrient transport under well-watered conditions, thereby accelerating overall plant growth [18]. Variations in water availability also induce changes in leaf cellular properties, including effects on cell membrane stability and permeability, as well as triggering cell wall remodeling, increased elasticity, and folding [19–22]. Under drought, plants utilize intracellular HCO_3 via carbonic anhydrase (CA) to generate carbon substrates and metabolic water, improving cellular water status and sustaining photosynthesis [23]. Additionally, osmolytes or cell volume adjustments further stabilize turgor pressure and leaf water potential, thereby modulating photosynthetic response trajectories [24, 25]. Aquaporins (AQPs) are key proteins for trans-membrane water movement, which facilitate rapid water exchange between the cytosol and vacuolar lumen, as well as between the cytosol and apoplast [26]. Studies have

shown that plasma-membrane intrinsic proteins (PIPs) and tonoplast intrinsic proteins (TIPs) jointly modulate cytosolic osmotic potential to maintain cell turgor [27]. The direction-independent regulation of transmembrane water transport by AQPs renders intracellular water dynamics complex and unpredictable, increasing the difficulty of accurately assessing plant water use characteristics. Timely monitoring of leaf cellular water dynamics is therefore essential. However, due to limitations of current detection techniques, research on the real-time dynamics of cellular water, nutrients, and energy remains constrained.

Plant electrical signal is defined as "any detectable fluctuation in potential, current, or resistance recordable from plant cells or tissues." Electrophysiological techniques enable real-time, online, high-sensitivity, and user-friendly monitoring; by rapidly capturing these signals, we can instantly assess how internal metabolic activities respond to external environmental changes [28]. The plant plasma membrane is a phospholipid bilayer embedded with integral or transmembrane proteins. Water crosses this membrane either through free diffusion or via AQPs. Due to its selective permeability to ions, the plasma membrane allows mesophyll cells to be modeled as a capacitor: the solutions on its two sides act as the plates, the membrane itself as the dielectric, and the cellular organelles as resistors. This configuration endows the entire cell with combined capacitive and resistive properties [29]. The permeability of leaf cells varies with external conditions, leading to coordinated changes in intracellular/extracellular ion concentrations, solute transport, and water status. These changes, in turn, induce an immediate shift in the recorded electrical signal. In previous studies, we successfully applied this electrophysiological technique to monitor intracellular water and nutrient status, using the acquired electrophysiological data to quantify transport capacity, physiological health, and plant stress resistance [30–32]. Therefore, by capturing the electrophysiological information of leaves under contrasting water conditions, we can rapidly characterize the dynamic responses of intracellular water, nutrients, and energy to changing water conditions. This approach enables instantaneous probing of plant-water relations at the cellular resolution, and discriminates the distinct water use patterns of *B. campestris* and *B. oleracea*.

Upon leaf detachment, the transpiration stream is disrupted, and the bulk flow of water within the apoplastic and symplastic pathways ceases almost instantaneously, effectively 'locking' the cellular water in its existing state. Wrapping the petiole in moist gauze minimizes further water loss, generating a "non-saturated" condition that closely mimics the plant's in-situ status. In contrast, immediate immersion of detached leaves in deionized water induces cellular water absorption and swelling, ultimately achieving a "fully-saturated" state characterized by balanced membrane influx and efflux. In this study, leaves of *B. campestris* and *B. oleracea* plants were subjected to both saturation treatments, and their electrophysiological parameters were measured. Based on the Nernst equation, characteristic parameters, including intracellular water and nutrient utilization, metabolic energy, and metabolic vitality, were derived. Additionally, the acceleration of intracellular water transport rate was defined and quantified. Comparisons between saturated and non-saturated conditions revealed species-specific differences in responses of leaf intracellular substances and energy. These findings provide quantitative water-use signatures to support the further studying of water saving irrigation of the two Brassicaceae plant species.

2 Materials and Methods

2.1 Experimental Materials and Treatments

The experiment was conducted in a greenhouse of Jiangsu Zhongxin Seed Technology Co., Ltd. located at 120°46′19.74″E, 31°52′43.53″N in Zhangjiagang, Jiangsu Province. *Brassica campestris* (hybrid 'Yungangxin 50') and *Brassica oleracea* (line 'Hubu') plants were both bred and grown in the greenhouse. *B. oleracea* seeds were sown in nursery trays and transplanted after 37 days; *B. campestris* was direct-seeded and later thinned. Each cultivar constituted one treatment. Basal fertilizer was applied once with no additional top-dressing; routine field management was practiced. All measurements were conducted in triplicate.

2.2 Measurement Methods

2.2.1 *Measurement and Calculation of Electrophysiological Parameters*

A schematic of the parallel-plate electrode configuration is shown in Figure 1. The system consists of two circular copper electrodes (diameter: 7 mm, thickness: 2 mm) mounted on insulating acrylic holders. Copper was selected as the electrode

material due to its excellent electrical conductivity and corrosion resistance, ensuring stable signal transmission during measurement. Plant tissues are characterized by low capacitance and high impedance. Copper sheets are used as contact electrodes, and resistance can be neglected for such high-impedance materials as plant leaves. Prior to each measurement session, the LCR meter (HIOKI 3532-50, Japan) was calibrated using the manufacturer's provided open-circuit and short-circuit compensation fixtures to eliminate systematic instrumental errors and parasitic impedances.

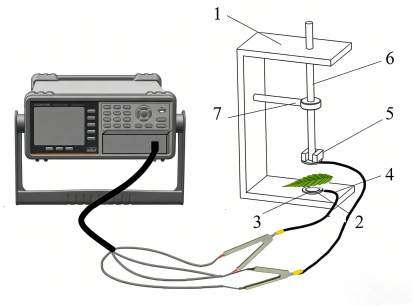

Figure 1. Schematic of the parallel-plate capacitor: 1: bracket, 2: foam board, 3: electrode; 4: wire, 5: iron, 6: plastic bar, 7: fixation clamp.

2.2.2 *Measurement and Calculation of Electrophysiological Parameters (Continued)*

Firstly, a parallel-plate capacitor was connected to an LCR meter (HIOKI 3532-50, Japan). A fresh leaf was excised, and its petiole was immediately wrapped with moist (non-saturated) gauze before being placed between the electrodes of the capacitor. The excitation voltage of 1.5 V at 3 kHz was selected based on voltage optimization tests, as demonstrated in our previous studies [33]. Different compressive forces ($F = 1.1, 2.1, 4.1, 6.1, 8.1$ N) were applied by adding 100 g brass weights (M). In parallel mode, the physiological capacitance (C), resistance (R) and impedance (Z) were recorded for each force level. For each treatment, measurements were performed at three distinct locations per leaf, with three replicate leaves tested. The detailed derivation and calculation procedures of the relevant electrophysiological parameters are provided in supplementary material (S1).

First, calculate the physiological capacitive reactance (X_C) from the measured capacitance (C). Subsequently, derive the physiological inductive reactance (X_L) using the R, Z and X_C. Finally, construct force-response models for the leaf electrophysiological parameters to obtain the model coefficients. These models are defined as equations describing the variation of physiological indices (C, R, Z, X_C and X_L) with compressive force F [34], as follows:

$$C = y_0 + k_0 F \tag{1}$$
$$R = y_1 + k_1 e^{-b_1 F} \tag{2}$$
$$Z = y_2 + k_2 e^{-b_2 F} \tag{3}$$
$$X_C = y_3 + k_3 e^{-b_3 F} \tag{4}$$
$$X_L = y_4 + k_4 e^{-b_4 F} \tag{5}$$

where y, k, and b are model parameters.

Using these parameters, calculate the leaf-specific effective thickness (d) and the intrinsic electrophysiological parameters (IC, IR, IZ, IX_C, IX_L) under the condition of $F = 0$, i.e.,

$$d = \frac{U^2 k_0}{2} \tag{6}$$
$$IR = y_1 + k_1 \tag{7}$$
$$IZ = y_2 + k_2 \tag{8}$$
$$IX_C = y_3 + k_3 \tag{9}$$
$$IX_L = y_4 + k_4 \tag{10}$$
$$IC = \frac{1}{2\pi f \times IX_C} \tag{11}$$

where U is the test voltage, and is equal to 1.5 V, $\pi = 3.1416$, f is the frequency, and is equal to 3 kHz.

On this basis, compute the leaf-cell water-use indices, including leaf intracellular water holding capacity (LIWHC), leaf intracellular water use efficiency (LIWUE), leaf intracellular water holding time (LIWHT), and leaf intracellular water transfer rate (LIWTR); as well as the nutrient-use indices: active nutrient transport capacity (NAT), passive nutrient transport capacity (NPT), low-nutrient tolerance capacity (RLN), and electrophysiological ion transport efficiency (EITE) [23, 35]. The calculation formulas for the above leaf intracellular water-use and nutrient-use parameters are presented below:

$$\mathrm{LIWHC} = \sqrt{\mathrm{IC}^3} \tag{12}$$

$$\mathrm{LIWUE} = \frac{d}{\mathrm{LIWHC}} \tag{13}$$

$$\mathrm{LIWHT} = \mathrm{IC} \times \mathrm{IZ} \tag{14}$$

$$\mathrm{LIWTR} = \frac{\mathrm{LIWHC}}{\mathrm{LIWHT}} \tag{15}$$

$$\mathrm{NAT} = \frac{\mathrm{IX}_L^{-1}}{\mathrm{IR}^{-1}} \tag{16}$$

$$\mathrm{NPT} = \frac{\mathrm{IX}_c^{-1}}{\mathrm{IR}^{-1}} \tag{17}$$

$$\mathrm{RLN} = \frac{100 \times \mathrm{NAT}}{\mathrm{NAT} + \mathrm{NPT}} \times 100\% \tag{18}$$

$$\mathrm{EITE} = \frac{100}{\mathrm{NAT} + \mathrm{NPT}} \tag{19}$$

It should be noted that EITE (Electrophysiological ion transport efficiency) used in this study is an electrophysiological proxy reflecting the overall resistance/efficiency of ion transport across the cell membrane (the reciprocal of total transport capacity). This is fundamentally different from the traditional agronomic concept of nutrient use efficiency (biomass production per unit nutrient). The changes observed during the 30-minute immersion primarily reflect membrane property adjustments (such as membrane expansion, ion channel activity changes, and electrolyte dilution) due to altered cell hydration status, rather than long-term metabolic electrophysiological ion transport efficiency.

The total nutrient transport capacity (TNTC) is calculated as:

$$\mathrm{TNTC} = \mathrm{NAT} + \mathrm{NPT} \tag{20}$$

Using the electrophysiological model parameters above, calculate the unit metabolizable energy of plant leaf cells based on physiological impedance (ΔG_{Z-E}) and the unit metabolizable energy of plant leaf cells based on physiological resistance (ΔG_{R-E}). Then, combined with the leaf-specific effective thickness d, obtain the metabolic energy of plant leaf cells based on physiological impedance (ΔG_Z) and the metabolizable energy of plant leaf cells based on physiological resistance (ΔG_R), and further calculate the plant leaf cells metabolize energy (ΔG_B) [36]. The formulas are listed as follows:

$$\Delta G_{Z-E} = \frac{\ln k_2 - \ln y_2}{b_2} \tag{21}$$

$$\Delta G_{R-E} = \frac{\ln k_1 - \ln y_1}{b_1} \tag{22}$$

$$\Delta G_Z = \Delta G_{Z-E} \times d \tag{23}$$

$$\Delta G_R = \Delta G_{R-E} \times d \tag{24}$$

$$\Delta G_B = \frac{\Delta G_Z + \Delta G_R}{2} \tag{25}$$

By integrating the above water-use parameters with the intrinsic electrophysiological indices, the following indices of relative metabolic vigor are obtained: leaf nutrient transfer rate (STR), active nutrient transport flow per unit leaf area (UAF), active nutrient transport capacity in leaves (NAC), leaf metabolic flow (MF), leaf metabolic rate (MR), and relative metabolic activity (MA) [37]. The formulas are as follows:

$$\mathrm{STR} = \frac{\mathrm{LIWHC}}{\mathrm{LIWHT}} \tag{26}$$

$$\mathrm{UAF} = \frac{X_C}{X_L} \tag{27}$$

$$\mathrm{NAC} = \mathrm{STR} \times \mathrm{UAF} \tag{28}$$

$$\mathrm{MF} = \frac{1}{\mathrm{IR} \times \mathrm{IZ} \times X_C \times X_L} \tag{29}$$

$$\mathrm{MR} = \mathrm{STR} \times \mathrm{NAC} \tag{30}$$

$$\mathrm{MA} = (\mathrm{MF} \times \mathrm{MR})^{1/6} \tag{31}$$

Fresh leaves were also collected and immediately immersed in distilled water for 30 min to achieve full saturation. To ensure that leaf cells approximate their natural state to the greatest extent and guarantee comparability among different plant species, a uniform 30-minute water saturation was applied to allow full cell hydration. The use of deionized water creates a water potential gradient to drive cellular hydration. When leaves are immersed in deionized water, the water potential of deionized water is higher than that of the cell sap, driving water molecules into the cells through the cell membrane, thereby achieving water saturation. After blotting off surface water, the same electrophysiological parameters were recorded under this saturated condition using identical procedures and indices as for the non-saturated condition.

Finally, the change rate of each parameter between the two hydration states was calculated with the following formula:

Table 1. Intrinsic electrophysiological parameters under saturated and non-saturated conditions.

Variety	Water condition	IC (pF)	IR (MΩ)	IZ (MΩ)	IX_c (MΩ)	IX_L (MΩ)
B. campestris	Saturated	264.096±43.200a	0.033±0.009b	0.031±0.007b	0.089±0.016b	0.109±0.020b
	Non-saturated	334.195±4.966a	0.211±0.023a	0.140±0.014ab	0.194±0.015b	0.338±0.035b
B. oleracea	Saturated	256.875±13.908a	0.132±0.023ab	0.108±0.011ab	0.209±0.029b	0.295±0.029b
	Non-saturated	96.667±20.771b	0.221±0.092a	0.198±0.074a	0.540±0.075a	0.675±0.134a

Note: Mean ± SE ($n = 3$) followed by different letters in the same column are significantly different at $P \leq 0.05$, according to one-way ANOVA.

$$\text{Change rate of electrophysiological parameter} = \frac{\text{Value}_{\text{saturated}} - \text{Value}_{\text{non-saturated}}}{\text{Value}_{\text{non-saturated}}} \times 100\% \quad (32)$$

where $\text{Value}_{\text{saturated}}$ and $\text{Value}_{\text{non-saturated}}$ represent the measured electrophysiological parameters under saturated and non-saturated conditions, respectively.

2.2.3 Definition and Calculation of Acceleration

In physics, the change in velocity is obtained by subtracting the initial velocity from the final velocity. Dividing this velocity change by the elapsed time yields the rate of velocity change per unit time, which is formally denoted as acceleration (a).

An external stimulus modifies membrane permeability, alters the extra- and intracellular electrolyte gradient, and thereby changes the rate of intracellular water transport. With the non-saturated condition designated as the initial velocity (v_0) and the saturated condition as the final velocity (v_s), and the immersion interval defined as t, the acceleration (a) of intracellular water transfer in leaves is defined as:

$$a = \frac{v_s - v_0}{t} \quad (33)$$

where a is acceleration, v_s is the intracellular water transfer rate of the leaf under saturated condition, v_0 is the intracellular water transfer rate of the leaf under non-saturated condition, and t is the immersion time, which is equal to 0.5 h in this experiment.

2.3 Statistical Analysis

Data were organized and summarized with Excel 2021, modelled with SigmaPlot 14.0, and plotted with Origin 2019. One-way ANOVA followed by Duncan's multiple-range test ($P \leq 0.05$) was performed in SPSS 14.0. Values are presented as means ± SE ($n = 3$). For each biological replicate ($n = 3$), measurements were performed at five distinct locations per leaf, with ten recordings per location. The average of 50 measurements per leaf was used as one biological replicate to minimize measurement errors and ensure representative sampling of the leaf's overall physiological state.

3 Results

3.1 Intrinsic Electrophysiological Parameters of *B. campestris* and *B. oleracea* Leaves

Table 1 shows that IR of *B. campestris* under non-saturated condition is significantly higher than that under saturated condition, whereas IC, IZ, IX_c and IX_L do not differ significantly between the two water conditions. IX_c and IX_L of *B. oleracea* are significantly higher under non-saturated condition than those under saturated condition. IC of *B. oleracea* under non-saturated condition is significantly lower than that under saturated condition, while IR and IZ show no difference between those two water conditions.

3.2 Water and Nutrient use Parameters of *B. campestris* and *B. oleracea* Leaves

According to Tables 2 and 3, *B. campestris* under non-saturated condition exhibited significantly higher values of LIWHC, LIWHT, NAT, NPT, and TNTC compared to those under saturated condition. In contrast, LIWUE, LIWTR, RLN, and EITE showed the opposite trend (i.e., higher values under saturated condition). For *B. oleracea*, no significant differences in LIWUE, LIWHT, LIWTR, NAT, NPT, EITE, or TNTC were detected between saturated and non-saturated conditions.

Compared with the non-saturated condition, the LIWTR of *B. campestris* and *B. oleracea* under saturated condition increased by 339.98% and 128.59%, respectively. Under saturation, *B. campestris* exhibited higher LIWUE, RLN and EITE, but lower LIWHC, LIWHT, NAT, NPT and TNTC; in contrast, *B. oleracea* showed the opposite trend. When shifting from the non-saturated to saturated condition, the acceleration of intracellular water transfer rate in *B. campestris* leaves

Table 2. Water use parameters under saturated and non-saturated conditions.

Variety	Water condition	LIWHC	LIWUE	LIWHT	LIWTR	a
B. campestris	Saturated	4375.985±1092.912b	0.163±0.049a	7.843±1.444c	584.541±136.513a	903.368
	Non-saturated	6110.423±135.928a	0.033±0.003b	46.801±4.691a	132.857±11.812b	
B. oleracea	Saturated	4126.137±330.514b	0.032±0.005b	27.761±3.304b	151.447±16.933b	170.388
	Non-saturated	2189.915±807.595b	0.071±0.017b	16.888±3.809bc	66.253±25.665b	
Change rate of electrophysiological parameters (%) in *B. campestris*		-28.385	393.939	-83.242	339.978	
Change rate of electrophysiological parameters (%) in *B. oleracea*		319.952	-54.930	64.383	128.589	

Note: Mean ± SE ($n = 3$) followed by different letters in the same column are significantly different at $P \leq 0.05$, according to one-way ANOVA.

Table 3. Nutrient use parameters under saturated and non-saturated conditions.

Variety	Water condition	NAT	NPT	RLN (%)	EITE	TNTC
B. campestris	Saturated	0.298±0.039b	0.364±0.057b	45.187±0.785a	158.616±26.115a	0.662±0.096b
	Non-saturated	0.624±0.004a	1.082±0.043a	36.608±0.792b	58.707±1.656b	1.706±0.047a
B. oleracea	Saturated	0.451±0.065b	0.661±0.149b	41.295±1.948a	96.93±18.449ab	1.112±0.214b
	Non-saturated	0.302±0.067b	0.383±0.111b	44.928±1.518a	163.733±34.020a	0.685±0.179b
Change rate of electrophysiological parameters (%) in *B. campestris*		-52.244	-66.359	23.435	170.182	-61.196
Change rate of electrophysiological parameters (%) in *B. oleracea*		49.338	72.585	-8.086	-40.800	62.336

Note: Mean ± SE ($n = 3$) followed by different letters in the same column are significantly different at $P \leq 0.05$, according to one-way ANOVA.

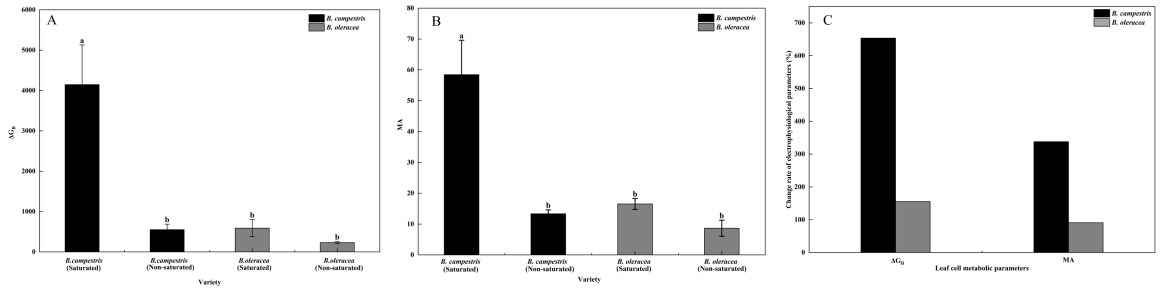

Figure 2. Leaf ΔG_B (A), MA (B) and change rate of ΔG_B and MA (C) under saturated and non-saturated water conditions. (Note: Values in the figure are presented as mean ± SE ($n = 3$). Based on the results of One-way ANOVA, different lowercase letters are labeled above the error bars for a given parameter when there are significant differences in values of that parameter between different groups at the P ≤ 0.05 level.).

was approximately five times that in *B. oleracea* leaves.

4 Leaf Cellular Metabolic Parameters of *B. campestris* and *B. oleracea*

Figure 2 demonstrates that both the ΔG_B and MA of *B. campestris* under saturated condition were significantly higher than those under non-saturated condition. In contrast, *B. oleracea* showed no significant differences in either parameter between the two water conditions. Compared with the non-saturated condition, saturated condition induced varying degrees of increase in ΔG_B and MA for both varieties: ΔG_B increased by 653.55% and 155.38%, while MA rose by 337.76% and 90.92% for *B. campestris* and *B. oleracea*, respectively. Notably, the increments of both parameters in *B. oleracea* were markedly lower than those in *B. campestris*.

5 Discussion

5.1 Discussion

According to the energy conservation principle, energy produced via photosynthesis under stress is primarily allocated to growth, cellular metabolism, and stress resistance [29]. Consequently, shifts in intracellular metabolite metabolism under varying water conditions directly impact photosynthesis and growth, while also regulating whole-plant water balance. In this experiment, the two Brassicaceae plant species displayed distinct response patterns under

both water conditions.

The growth of *B. campestris* is significantly influenced by the water conditions [38, 39]. *B. campestris* has pointed leaves, rapid growth, and high water demand, thus showing a distinct response to water changes. The firmness of *B. campestris* is related to the cellulose content in the epidermis of the flower stalk. *B. campestris* has tender, thin leaves with relatively low firmness and weak water retention capacity, resulting in rapid water loss [40]. Under saturated water condition, the intracellular water transport rate of *B. campestris* leaves was high, with LIWTR increasing by 339.98% compared to non-saturated condition. This reduced the cell water-holding time and significantly decreased LIWHT. Although nutrient transport in the leaves was restricted, the efficient transport and utilization of intracellular water enhanced a higher EITE value. Leaf cells exhibited higher MA and ΔG_B values under this condition compared to those under non-saturated conditions. The higher ΔG_B value indicated that greater cellular energy could be potentially used for growth or other metabolisms. The non-saturated water condition was closer to the actual growth environment of plants. Under this condition, the IR of *B. campestris* leaves was significantly higher than that in the saturated condition with poor leaf water conductance and a marked decrease in LIWTR. However, its LIWHT was higher, as leaf cells reduced water transport rate to extend intracellular water retention time. The high resistance to material transport within cells increased energy consumption during substance transfer, resulting in lower EITE and significant reductions in cellular metabolic energy and vitality.

B. oleracea leaves are thicker, with slow water loss and strong water retention. Therefore, the changes in intracellular water retention, utilization, and transport of *B. oleracea* leaves under both saturated and non-saturated water conditions were relatively small. Total nutrient transport and metabolism remained stable, with no significant changes in leaf cell metabolic energy and vitality.

The acceleration (a) of intracellular water transfer rate provides a dynamic metric for cellular hydration kinetics. Based on the classical physics concept of acceleration $(a = \Delta v/\Delta t)$, we applied it to plant water physiology by defining the initial velocity (v_0) as LIWTR under non-saturated condition, the final velocity (v_s) as LIWTR under saturated condition, and the time interval (Δt) as the 30-minute immersion period. Thus, acceleration (a) quantifies the rapidity with which leaf cells alter their water transport kinetics in response to changed water availability, serving as a metric for cellular hydration responsiveness. The markedly higher a value in *B. campestris* (903.37) compared to *B. oleracea* (170.39) reveals a fundamental difference in responsiveness, suggesting superior kinetic agility in *B. campestris* potentially attributable to species-specific differences in aquaporin regulation or membrane properties governing water permeability.

When comparing the change rates from non-saturated to saturated water conditions, the increase in LIWHC of *B. campestris* was significantly lower than that of *B. oleracea*. However, its high acceleration facilitated intracellular water transfer, resulting in a LIWTR increase approximately five times greater than that of *B. oleracea*. The sharp elevation in ΔG_B underpins efficient water utilization and transport in saturated *B. campestris* leaves, indicating a more sensitive water-use response. In contrast, *B. oleracea* exhibited robust water-retention capacity: its intracellular water transfer rate increased only moderately upon saturation (attributed to low a value), and ΔG_B rose slightly, an adaptation that stabilized intracellular water and nutrient levels, reflecting robust internal regulatory mechanisms and high environmental adaptability. Consequently, saturated water condition exerted minimal impact on the relative metabolic activity of *B. oleracea*. Overall, compared with *B. campestris*, *B. oleracea* demonstrated superior drought tolerance, lower water sensitivity, and enhanced capacity to cope with external environmental stimuli.

The contrasting LIWUE responses reveal fundamentally different water-use strategies at the cellular level. *B. campestris* exhibited a "high-response" strategy: under saturated conditions, LIWUE increased by 393.9%, indicating high sensitivity to water availability and an "opportunistic" strategy when water is plentiful. In contrast, *B. oleracea* displayed a "conservative" strategy: LIWUE remained relatively stable regardless of water conditions (non-significant decrease), suggesting robust internal regulatory mechanisms and higher adaptability to environmental fluctuations. This aligns with the acceleration results: *B. campestris* $(a = 903.37)$ showed approximately five-fold higher responsiveness than *B. oleracea* $(a = 170.39)$.

After 30 minutes of immersion, the leaves reached full saturation. The aforementioned analyses demonstrate that, overall, all parameter values under

saturated water condition are superior to those under non-saturated water condition. To enable direct interspecific comparison, maintaining leaves in a saturated state minimizes environment-induced variability in electrophysiological measurements. Consequently, the acquired data optimally reflect the intrinsic characteristics and potential of each plant species.

By comparing the saturated-condition electrophysiological parameters of the two plant species, and evaluating the change rate of LIWHC, LIWUE, LIWTR, ΔG_B, and MA, coupled with the acceleration of intracellular water transfer, *B. campestris* exhibited superior intracellular water delivery compared to *B. oleracea*. It also possessed higher cellular metabolic energy and activity. During the transition from non-saturated to saturated water conditions, *B. campestris* displayed smaller variations in intracellular water-holding capacity and retention time, but more rapid changes in water-use and transfer rates. These findings indicated that *B. campestris* had higher water sensitivity than *B. oleracea*.

6 Conclusion

Under saturated water conditions, *B. campestris* leaves exhibited rapid intracellular water utilization and transfer, high EITE, strong tolerance to low nutrients, and vigorous metabolic activity; the opposite was observed under non-saturated water condition. In contrast, *B. oleracea* leaves maintained a slightly longer intracellular water-holding duration, stable nutrient transport, and steady cellular metabolism when saturated. Both plant species thus displayed enhancing intracellular physiological activity in the saturated water condition, where the electrophysiological parameters could accurately reflect their intrinsic traits and potential. From non-saturated to saturated water conditions, *B. campestris* showed smaller increases in intracellular water-holding capacity and duration but more rapid changes in water utilization and transfer rates, whereas *B. oleracea* exhibited the reverse pattern. Therefore, compared with *B. oleracea*, *B. campestris* had greater sensitivity to water changes. The results demonstrate that electrophysiological methods can serve as a rapid, non-invasive diagnostic tool for assessing crop water response characteristics at the cellular level, providing theoretical basis and technical support for drought-tolerant variety screening.

However, the use of detached leaves in this study had some limitations in reflecting plant water demand. While this approach allows for precise control over water status and isolation of cellular responses from whole-plant systemic signals, it inherently excludes the complex regulatory networks involving root-shoot communication and long-distance vascular transport. Consequently, the findings primarily reflect the intrinsic water response capacity at the leaf cellular level. Extrapolation to whole-plant water demand characteristics in agricultural settings should be done cautiously and requires validation through integrated whole-plant physiological studies.

Data Availability Statement

Data will be made available on request.

Funding

This work was supported by the Priority Academic Program Development of Jiangsu Higher Education Institutions under Grant PAPD-2023-87.

Conflicts of Interest

The authors declare no conflicts of interest.

AI Use Statement

The authors declare that no generative AI was used in the preparation of this manuscript.

Ethical Approval and Consent to Participate

Not applicable.

References

[1] Zhang, H., Cun, Y., Wang, J., Wu, M., Li, X., Liang, Q., ... & Deng, J. (2022). Acetylsalicylic acid and salicylic acid alleviate postharvest leaf senescence in Chinese flowering cabbage (Brassica rapa var. parachinensis). *Postharvest Biology and Technology, 194*, 112070. [CrossRef]

[2] Akter, A., Akhter, S., & Hossain, M. M. (2025). Water stresses alter the growth, yield and quality of broccoli (Brassica Oleracea var. italica). *Scientific Reports, 15*(1), 40107. [CrossRef]

[3] Lin, Y., Liu, S., Fang, X., Ren, Y., You, Z., Xia, J., ... & Shangguan, L. (2023). The physiology of drought stress in two grapevine cultivars: Photosynthesis, antioxidant system, and osmotic regulation responses. *Physiologia Plantarum, 175*(5), e14005. [CrossRef]

[4] Biswas, D., Gjetvaj, B., St. Luce, M., Liu, K., & Asgedom, H. (2023). Effects of soil water and nitrogen on drought resilience, growth, yield, and grain quality of a spring wheat. *Canadian Journal of Plant Science, 103*(4), 401-410. [CrossRef]

[5] Hilário, S., Pinto, G., Monteiro, P., Santos, L., & Alves, A. (2023). The impact of two Diaporthe species on Vaccinium corymbosum physiological performance under different water availability scenarios. *European Journal of Plant Pathology, 166*(2), 161-177. [CrossRef]

[6] Duan, H., Shao, C., Luo, X., Resco de Dios, V., Tissue, D. T., & Ding, G. (2023). Root relative water content is a potential signal for impending mortality of a subtropical conifer during extreme drought stress. *Plant, Cell & Environment, 46*(9), 2763-2777. [CrossRef]

[7] Pereira, T. S., Oliveira, L. A., Andrade, M. T., Haverroth, E. J., Cardoso, A. A., & Martins, S. C. (2024). Linking water-use strategies with drought resistance across herbaceous crops. *Physiologia Plantarum, 176*(1), e14114. [CrossRef]

[8] Qin, J., Si, J., Jia, B., Zhao, C., Zhou, D., He, X., ... & Zhu, X. (2023). Water use strategies of Nitraria tangutorum in the lake-basin region of the Badain Jaran Desert. *Frontiers in Plant Science, 14*, 1240656. [CrossRef]

[9] Xing, D., Mao, R., Li, Z., Wu, Y., Qin, X., & Fu, W. (2022). Leaf intracellular water transport rate based on physiological impedance: A possible role of leaf internal retained water in photosynthesis and growth of tomatoes. *Frontiers in Plant Science, 13*, 845628. [CrossRef]

[10] Ahmed, S., Kouser, S., Asgher, M., & Gandhi, S. G. (2021). Plant aquaporins: A frontward to make crop plants drought resistant. *Physiologia Plantarum, 172*(2), 1089–1105. [CrossRef]

[11] Kou, J., Yan, D., Qin, B., Zhou, Q., Liu, C., & Zhang, L. (2023). Physiological response mechanism of European birch (Betula pendula Roth) to PEG-induced drought stress and hydration. *Frontiers in Plant Science, 14*, 1226456. [CrossRef]

[12] Lai, Z., Zhang, K., Liao, Z., Kou, H., Pei, S., Dou, Z., ... & Fan, J. (2023). Stem hydraulic conductance, leaf photosynthesis, and carbon metabolism responses of cotton to short-term drought and rewatering. *Agronomy, 14*(1), 71. [CrossRef]

[13] Zhang, X. M., Duan, S. G., Xia, Y., Li, J. T., Liu, L. X., Tang, M., ... & Yi, Y. (2023). Transcriptomic, physiological, and metabolomic response of an alpine plant, Rhododendron delavayi, to waterlogging stress and post-waterlogging recovery. *International Journal of Molecular Sciences, 24*(13), 10509. [CrossRef]

[14] Beegum, S., Truong, V., Bheemanahalli, R., Brand, D., Reddy, V., & Reddy, K. R. (2023). Developing functional relationships between waterlogging and cotton growth and physiology-towards waterlogging modeling. *Frontiers in Plant Science, 14*, 1174682. [CrossRef]

[15] Qu, Z., Qi, X., Liu, Y., Liu, K., & Li, C. (2020). Interactive effect of irrigation and polymer-coated potassium chloride on tomato production in a greenhouse. *Agricultural Water Management, 235*, 106149. [CrossRef]

[16] Li, S., Yang, L., Huang, X., Zou, Z., Zhang, M., Guo, W., ... & Zhou, L. (2023). Mineral nutrient uptake, accumulation, and distribution in Cunninghamia lanceolata in response to drought stress. *Plants, 12*(11), 2140. [CrossRef]

[17] Song, H., Miao, Z., Jiang, G., Zhang, Y., Lu, F., Deng, F., ... & Zhao, F. (2022). Relationships between the water uptake and nutrient status of rubber trees in a monoculture rubber plantation. *Agronomy, 12*(9), 1999. [CrossRef]

[18] Zhang, F., Zhao, Y., Zhang, Y., Shi, Y., Hou, L., Khan, A., ... & Zhang, Y. (2024). Mechanism of exogenous silicon in enhancing cold stress tolerance in Solanum lycopersicum L. seedlings: insights from resistance and quality indicators. *Horticulturae, 11*(1), 4. [CrossRef]

[19] Shaaban, A., Mahfouz, H., Megawer, E. A., & Saudy, H. S. (2023). Physiological changes and nutritional value of forage clitoria grown in arid agro-ecosystem as influenced by plant density and water deficit. *Journal of Soil Science and Plant Nutrition, 23*(3), 3735-3750. [CrossRef]

[20] Bagheri, H., Hashemabadi, D., Eslam, B. P., & Sedaghathoor, S. (2023). Effects of zinc-nano oxide, salicylic acid and sodium nitroprusside on physiological properties, antioxidant enzyme activities and secondary metabolites of Viola odorata under drought stress. *Acta Scientiarum Polonorum Hortorum Cultus, 22*(6), 29–41. [CrossRef]

[21] Tikhomirova, T. S., Krutovsky, K. V., & Shestibratov, K. A. (2023). Molecular traits for adaptation to drought and salt stress in birch, oak and poplar species. *Forests*, 14(1), 7. [CrossRef]

[22] Ahl, L. I., Mravec, J., Jørgensen, B., Rudall, P. J., Rønsted, N., & Grace, O. M. (2019). Dynamics of intracellular mannan and cell wall folding in the drought responses of succulent Aloe species. *Plant, cell & environment, 42*(8), 2458-2471. [CrossRef]

[23] Polishchuk, O. V. (2021). Stress-related changes in the expression and activity of plant carbonic anhydrases. *Planta, 253*(2), 58. [CrossRef]

[24] Cao, S., Yang, F., Zhang, H., Wang, Q., Xu, G., Zhu, B., & Wu, C. (2023). Physiological and transcriptome profiling analyses reveal important roles of Streptomyces rochei D74 in improving drought tolerance of Puccinellia distans (Jacq.) Parl. *Environmental and Experimental Botany, 207*, 105204. [CrossRef]

[25] Vogler, H., Burri, J. T., Nelson, B. J., & Grossniklaus, U. (2020). Simultaneous measurement of turgor pressure and cell wall elasticity in growing pollen tubes. In *Methods in cell biology* (Vol. 160, pp. 297-310). Academic Press. [CrossRef]

[26] Rahman, A., Kawamura, Y., Maeshima, M., Rahman, A., & Uemura, M. (2020). Plasma membrane aquaporin members PIPs act in concert to regulate

cold acclimation and freezing tolerance responses in Arabidopsis thaliana. *Plant and Cell Physiology, 61*(4), 787–802. [CrossRef]

[27] Kapilan, R., Vaziri, M., & Zwiazek, J. J. (2018). Regulation of aquaporins in plants under stress. *Biological Research*, 51(1), 4. [CrossRef]

[28] Fromm, J., & Lautner, S. (2007). Electrical signals and their physiological significance in plants. *Plant, Cell & Environment, 30*(3), 249–257. [CrossRef]

[29] Zhang, C., Wu, Y., Su, Y., Xing, D., Dai, Y., Wu, Y., & Fang, L. (2020). A plant's electrical parameters indicate its physiological state: A study of intracellular water metabolism. *Plants, 9*(10), 1256. [CrossRef]

[30] Zhang, C., Su, Y., Wu, Y., Li, H., Zhou, Y., & Xing, D. (2021). Comparison on the nutrient plunder capacity of Orychophragmus violaceus and Brassica napus L. based on electrophysiological information. *Horticulturae, 7*(8), 206. [CrossRef]

[31] Zhao, X., Wu, Y., Xing, D., Li, H., & Zhang, F. (2023). Water metabolism of Lonicera japonica and Parthenocissus quinquefolia in response to heterogeneous simulated rock outcrop habitats. *Plants, 12*(12), 2279. [CrossRef]

[32] Xing, D., Wang, W., Wu, Y., Qin, X., Li, M., Chen, X., & Yu, R. (2022). Translocation and Utilization Mechanisms of Leaf Intracellular Water in Karst Plants Orychophragmus violaceus (L.) OE Schulz and Brassica napus L. *Horticulturae, 8*(11), 1082. [CrossRef]

[33] Najdenovska, E., Dutoit, F., Tran, D., Plummer, C., Wallbridge, N., Camps, C., & Raileanu, L. E. (2021). Classification of plant electrophysiology signals for detection of spider mites infestation in tomatoes. *Applied Sciences, 11*(4), 1414. [CrossRef]

[34] Zhang, C., Wu, Y., Su, Y., Li, H., Fang, L., & Xing, D. (2021). Plant's electrophysiological information manifests the composition and nutrient transport characteristics of membrane proteins. *Plant signaling & behavior, 16*(7), 1918867. [CrossRef]

[35] Li, H., Lv, J., Su, Y., & Wu, Y. (2023). Appropriate sodium bicarbonate concentration enhances the intracellular water metabolism, nutrient transport and photosynthesis capacities of Coix lacryma-jobi L. *Agronomy, 13*(7), 1790. [CrossRef]

[36] Chen, T., Wu, Y., Xing, D., & Duan, R. (2022). Effects of NaHSO3 on Cellular Metabolic Energy, Photosynthesis and Growth of Iris pseudacorus L. *Horticulturae, 8*(2), 185. [CrossRef]

[37] Ríos-Rojas, L., Tapia, F., & Gurovich, L. A. (2014). Electrophysiological assessment of water stress in fruit-bearing woody plants. *Journal of plant physiology, 171*(10), 799-806. [CrossRef]

[38] Li, J., Zhao, X., Nishimura, Y., & Fukumoto, Y. (2010). Correlation between bolting and physiological properties in Chinese cabbage (Brassica rapa L. pekinensis group). *Journal of the Japanese Society for Horticultural Science, 79*(3), 294-300. [CrossRef]

[39] Jang, Y., Kim, J., Lee, J., Lee, S., Jung, H., & Park, G. H. (2024). Drought tolerance evaluation and growth response of Chinese cabbage seedlings to water deficit treatment. *Agronomy, 14*(2), 279. [CrossRef]

[40] Zhu, J., Cai, D., Wang, J., Cao, J., Wen, Y., He, J., ... & Zhang, S. (2021). Physiological and anatomical changes in two rapeseed (Brassica napus L.) genotypes under drought stress conditions. *Oil Crop Science, 6*(2), 97-104. [CrossRef]

Appendix

The derivation formula of internal relationship between electrophysiological parameters and gripping force, and the derivation formula of leaf intracellular water and nutrient related indices and cellular metabolic energy.

A The intrinsic mechanism relationship between clamping force (F) and leaf R, Z, XC, XL and C

The Nernst equation can be used to describe the changes in the concentration of ions, ion groups and electric dipoles inside and outside of the cell membrane of a single cell. In parallel mode, the electrical properties of a single cell can be used to represent the overall electrical characteristics of the leaf. The impedance (Z) depends on the concentration of ions inside and outside the membrane and follows the Nernst equation, which is expressed as follows:

$$E - E^0 = \frac{R_0 T}{n_z F_0} \ln \frac{Q_i}{Q_0} \tag{S.1}$$

where E is the electromotive force (V), E^0 is the standard electromotive force (V), R_0 is the gas constant (8.31 J·K^{-1}·mol^{-1}), T is the thermodynamic temperature (K), Q_i is the concentration of electrolytes that respond to Z inside the cell membrane (mol·L^{-1}), Q_0 is the concentration of electrolytes that respond to Z outside the cell membrane (mol·L^{-1}), F_0 is the Faraday constant (9.65 × 10^4 C·mol^{-1}), and n_z is the number of transferred electrolytes (mol).

The internal energy of the electromotive force can be converted into pressure work, and they have a direct relationship, $PV = aE$, that is:

$$PV = aE = aE^0 + \frac{aR_0 T}{n_z F_0} \ln \frac{Q_i}{Q_0} \tag{S.2}$$

where P is the pressure intensity on the leaf cells (Pa), a is the transfer coefficient from electromotive force to energy, and V is the cell volume (m^3).

The pressure P applied to plant cells can be calculated using the pressure formula:

$$P = \frac{F}{S} \tag{S.3}$$

where F is the gripping force (N) and S is the effective area of the electrode plate (m^2). F can be calculated by the gravity formula:

$$F = (M + m)g \tag{S.4}$$

where M is the iron block mass (kg), m is the mass of the plastic rod and the plate electrode (kg), and $g = 9.8$ N/kg.

For mesophyll cells, the sum of Q_0 and Q_i is constant. Q_i is directly proportional to the conductivity of electrolytes that respond to Z, and the conductivity is the reciprocal of Z. Hence,

$$\frac{Q_i}{Q_0} \tag{S1}$$

can be expressed as

$$\frac{Q_i}{Q_0} = \frac{\frac{J_0}{Z}}{Q - \frac{J_0}{Z}} \tag{S.5}$$

where J_0 is the transfer coefficient between Q_i and Z, and $Q = Q_0 + Q_i$. Therefore, formula (S.2) was transformed into formula (S.6):

$$\frac{V}{S}F = aE^0 - \frac{aR_0T}{n_zF_0}\ln\frac{QZ - J_0}{J_0} \tag{S.6}$$

Formula (S.6) was rewritten:

$$\frac{aR_0T}{n_zF_0}\ln\frac{QZ - J_0}{J_0} = aE^0 - \frac{V}{S}F \tag{S.7}$$

and

$$\ln\frac{QZ - J_0}{J_0} = \frac{n_zF_0E^0}{R_0T} - \frac{Vn_zF_0}{SaR_0T}F \tag{S.8}$$

Formula (S.8) takes the exponents of both sides:

$$\frac{QZ - J_0}{J_0} = e^{\frac{n_zF_0E^0}{R_0T}}e^{\left(-\frac{Vn_zF_0}{SaR_0T}\right)F} \tag{S.9}$$

Further:

$$Z = \frac{J_0}{Q} + \frac{J_0}{Q}e^{\frac{n_zF_0E^0}{R_0T}}e^{\left(-\frac{Vn_zF_0}{SaR_0T}\right)F} \tag{S.10}$$

where Z is the leaf physiological impedance (MΩ).

Because $d = \frac{V}{S}$, formula (S.8) was transformed into:

$$Z = \frac{J_0}{Q} + \frac{J_0}{Q}e^{\frac{n_zF_0E^0}{R_0T}}e^{\left(-\frac{dn_zF_0}{aR_0T}F\right)} \tag{S.11}$$

For the same leaf tested in the same environment, d, a, E^0, R_0, T, n_z, F_0, Q, and J_0 of formula (S.10) are constant. Let $y_2 = \frac{J_0}{Q}$, $k_2 = \frac{J_0}{Q}e^{\frac{n_zF_0E^0}{R_0T}}$, and $b_2 = \frac{dn_zF_0}{aR_0T}$, and the intrinsic mechanism relationships of leaf Z and F were:

$$Z = y_2 + k_2e^{-b_2F} \tag{S.12}$$

where y_2, k_2, and b_2 are model parameters.

The leaf physiological capacitive reactance (X_C) was calculated according to formula (S.13):

$$X_C = \frac{1}{2\pi f \times C} \tag{S.13}$$

where C is the leaf physiological capacitance (pF).

The leaf physiological inductive reactance (X_L) was calculated according to formula (S.14):

$$-\frac{1}{X_L} = \frac{1}{Z} - \frac{1}{R} - \frac{1}{X_C} \tag{S.14}$$

With the same Z, the intrinsic mechanism relationships of leaf physiological resistance (R), X_C, X_L and F are revealed:

$$R = y_1 + k_1e^{-b_1F} \tag{S.15}$$

$$X_C = y_3 + k_3e^{-b_3F} \tag{S.16}$$

$$X_L = y_4 + k_4e^{-b_4F} \tag{S.17}$$

The derivative of formula (S.12) is as follows:

$$Z' = -b_2k_2e^{-b_2F} \tag{S.18}$$

According to formula (S.12), when $F = 0$, the intrinsic impedance (IZ) of the plant leaves could be obtained:

$$IZ = y_2 + k_2 \tag{S.19}$$

With the same IZ, when $F = 0$, the intrinsic resistance (IR), intrinsic capacitive reactance (IX_C), and intrinsic inductive reactance (IX_L) of plant leaves could be calculated as:

$$IR = y_1 + k_1 \tag{S.20}$$
$$IX_C = y_3 + k_3 \tag{S.21}$$
$$IX_L = y_4 + k_4 \tag{S.22}$$

The intrinsic capacitance (IC) of plant leaves could also be obtained:

$$IC = \frac{1}{2\pi f \times IX_C} \tag{S.23}$$

where $\pi = 3.1416$, f is the frequency, and IX_C is the intrinsic capacitive reactance.

According to the first law of thermodynamics, the work done by the clamping force obeys the Gibbs free energy equation:

$$\Delta G = \Delta H + PV \tag{S.24}$$

where ΔG is the Gibbs free energy (J), ΔH is the internal energy of the leaf cell system (J), P is the pressure intensity of the leaf cells (Pa), and V is the cell volume (m^3). P can be calculated by the pressure intensity formula:

$$P = \frac{F}{S} \tag{S.25}$$

where F is the clamping force (N) and S is the effective area of the electrode plate (m^2).

Mesophyll cells can be regarded as concentric sphere capacitors, and the capacitor energy is:

$$W = \frac{1}{2}U^2C \tag{S.26}$$

where W is the capacitor energy (J), and U is the test voltage (V).

According to energy conservation theory, the capacitor energy is equal to the work converted by Gibbs free energy, i.e., $W = \Delta G$. The leaf C and F relationship model was obtained:

$$C = \frac{2\Delta H}{U^2} + \frac{2V}{SU^2}F \tag{S.27}$$

It is assumed that d represents the specific effective thickness of the plant leaves; therefore, $d = \frac{V}{S}$. Formula (S.26) was transformed into formula (S.28):

$$C = \frac{2\Delta H}{U^2} + \frac{2d}{U^2}F \tag{S.28}$$

Let $y_0 = \frac{2\Delta H}{U^2}$, $k_0 = \frac{2d}{U^2}$, and formula (S.28) was transformed into formula (S.29):

$$C = y_0 + k_0F \tag{S.29}$$

Formula (S.29) is a linear model, where y_0 and k_0 are the model parameters.

As $k_0 = \frac{2d}{U^2}$, the specific effective thickness (d) of the plant leaves could be calculated as:

$$d = \frac{U^2k_0}{2} \tag{S.30}$$

B Calculation of leaf intracellular water use indices

The cell is a spherical structure, and its growth is closely related to the increased volume. The C of plant leaf cells can be calculated by a formula for concentric spherical capacitors:

$$C_c = \frac{4\pi\varepsilon R_1R_2}{R_2 - R_1} \tag{S.31}$$

where $\pi = 3.1416$, C_c is the capacitance of the concentric spherical capacitor (pF), ε is the dielectric constant of electrolytes, R_1 is the outer sphere radius (m), and R_2 is the inner sphere radius (m). For a plant cell, $R_2 - R_1$ is the thickness of the cell membrane. $R_1 \approx R_2$, as well as ε, and the thickness of the cell membrane is constant. Therefore, the cell volume (V_c) has the following relationship with cell's C_c:

$$V_c = \alpha\sqrt{C^3} \tag{S.32}$$

The cell volume is positively correlated with the volume of vacuoles, and the main component of the vacuole and cytoplasm is water. In other words, the water-holding capacity of cells is directly

proportional to $\sqrt{C^3}$. Therefore, $\sqrt{C^3}$ can represent the water-holding capacity of plant leaves. The leaf intracellular water-holding capacity (LIWHC) of plant leaves was obtained according to formula (S.32):

$$\text{LIWHC} = \sqrt[3]{C^3} \tag{S.33}$$

The specific effective thickness (d) of plant leaves represents cell growth, and the water-holding capacity supports plant cell growth. Therefore, the leaf intracellular water-use efficiency (LIWUE) of leaves was represented by formula (S.34):

$$\text{LIWUE} = \frac{d}{\text{LIWHC}} \tag{S.34}$$

According to Ohm's law, $I_Z = \frac{U}{Z}$, where I_Z is the physiological current (A). At the same time, the current is equal to the product of the capacitance and the differential of voltage in time, as shown in formula (S.35):

$$I_Z = IC \times \int dU \tag{S.35}$$

After the integral transformation, the current time is the product of C and Z. Therefore, the leaf intracellular water-holding time (LIWHT) of plant leaves is represented by formula (S.36):

$$\text{LIWHT} = IC \times IZ \tag{S.36}$$

And the leaf intracellular water transfer rate (LIWTR) is calculated as follows:

$$\text{LIWTR} = \frac{\text{LIWHC}}{\text{LIWHT}} \tag{S.37}$$

C Calculation of leaf intracellular nutrient transfer parameters

Plant cells have electrical properties of low C and high R, and it could be assumed that electrical cells were connected in parallel manner, and various aligned mesophyll cells make up the leaf capacitor. The value of IR in plant leaf cells can be measured as follows:

$$\frac{1}{\text{IR}} = \frac{1}{\text{IR}_1} + \frac{1}{\text{IR}_2} + \frac{1}{\text{IR}_3} + \cdots + \frac{1}{\text{IR}_n} \tag{S.38}$$

We can assume that the resistance of inside and outside membrane is equal; then, IR_1, IR_2, IR_3, and IR_n can represent inherent resistance of each unit cell membrane. Hence, the IR of the plant leaves were obtained as follows:

$$\frac{1}{\text{IR}} = \frac{n}{\text{IR}_0} \tag{S.39}$$

Further, the R of the cell membrane is closely related to lipids and proteins; therefore, n can be denoted as the relative number of lipids and proteins that induce membrane R in plant leaves.

Finally, the leaf IX_C in plant were measured as follows:

$$\frac{1}{\text{IX}_C} = \frac{p}{\text{IX}_{CO}} \tag{S.40}$$

As we know that X_C of cell membrane is closely related to the surface proteins, then IX_C or p was considered as the relative amount of surface proteins. Therefore, IX_C is inversely proportional to p.

$$\frac{1}{\text{IX}_L} = \frac{q}{\text{IX}_{LO}} \tag{S.41}$$

As we know that X_L of cell membrane is closely related to the conjugated proteins, then IX_L or q was considered as the relative number of conjugated proteins. Therefore, IX_L is inversely proportional to q.

The cell membrane proteins are most closely related to nutrient transport. The proportion of phospholipids, surface proteins (peripheral proteins) and conjugated proteins (intrinsic proteins) on the cell membrane strongly affects the transport capacity of cellular substances, and ultimately affects the nutrient transport efficiency of plants. Some non-selective ion channels (including intrinsic and extrinsic proteins), with extrinsic proteins playing a dominant role, allow ions to pass through the cell membrane along the electrochemical gradient, affecting the passive transport rate.

Among them, the leaf intracellular passive nutrient transport capacity (NPT) is calculated as follows:

$$\text{NPT} = \frac{p}{n} = \frac{I_{X_C}^{-1}}{I_R^{-1}} \tag{S.42}$$

In addition, the proportion of conjugated protein (intrinsic protein) is closely related to the active transport of nutrients. The proportion of cell nutrient transport capacity caused by these proteins

to total material transport capacity determines the leaf intracellular active nutrient transport capacity (NAT). Therefore, the calculation formula is as follows:

$$\mathrm{NAT} = \frac{q}{n} = \frac{I_{X_L}^{-1}}{I_R^{-1}} \tag{S.43}$$

Thus, the total nutrient transport capacity (TNTC) could be represented by equation (S.44):

$$\mathrm{TNTC} = \mathrm{NAT} + \mathrm{NPT} \tag{S.44}$$

Since the active transport capacity of plants determines the minimum concentration for ion uptake, it also determines the plant's tolerance to low-nutrient conditions. Therefore, the plant's low-nutrient tolerance can be represented by the ratio of its active transport capacity to its total nutrient transport capacity.

The low-nutrient tolerance capacity (RLN) is calculated as follows:

$$\mathrm{RLN} = \frac{100 \times \mathrm{NAT}}{\mathrm{NAT} + \mathrm{NPT}} \times 100\% \tag{S.45}$$

And then the electrophysiological ion transport efficiency (EITE) can be calculated as:

$$\mathrm{EITE} = \frac{100}{\mathrm{NAT} + \mathrm{NPT}} \tag{S.46}$$

D Calculation of leaf cellular metabolic energy

Cellular metabolic energy represents an additional form of energy input, distinct from the energy captured through photosynthesis. Based on the C, Z, R, X_C, X_L of plant leaves, the model constructed according to electrophysiological parameters can calculate the cellular metabolic energy of plant leaf.

Equation (S.12) leads to $Z = y_2 + k_2 e^{-b_2 F}$; where $y_2 = \frac{J_0}{Q}$, $k_2 = \frac{J_0 e^{\frac{n_z F_0 E^0}{R_0 T}}}{Q}$, and $b_2 = \frac{d n_z F_0}{a R_0 T}$. We take y_2 and b_2 and substitute it for k_2:

$$k_2 = y_2 e^{\frac{a E^0 b_2}{d}} \tag{S.47}$$

Further:

$$\frac{a E^0}{d} = \Delta G_{Z-E} \tag{S.48}$$

Equation (S.48) was deformed to obtain the unit cellular metabolic energy of plant leaf cells based on Z (ΔG_{Z-E}):

$$\Delta G_{Z-E} = \frac{\ln k_2 - \ln y_2}{b_2} \tag{S.49}$$

Additionally, equation (S.30) gives $d = \frac{U^2 k_0}{2}$. According to ΔG_{Z-E} and d, the cellular metabolic energy of plant based on Z (ΔG_Z) was obtained:

$$\Delta G_Z = \frac{\ln k_2 - \ln y_2}{b_2} \times d \tag{S.50}$$

Similarly, according to the model of R with F, the unit cellular metabolic energy of plant leaf cells based on R (ΔG_{R-E}) can be obtained:

$$\Delta G_{R-E} = \frac{\ln k_1 - \ln y_1}{b_1} \tag{S.51}$$

According to ΔG_{R-E} and d, the cellular metabolic energy of plant based on R (ΔG_R) was obtained:

$$\Delta G_R = \frac{\ln k_1 - \ln y_1}{b_1} \times d \tag{S.52}$$

The plant leaf cells metabolize energy (ΔG_B) is calculated as:

$$\Delta G_B = \frac{\Delta G_Z + \Delta G_R}{2} \tag{S.53}$$

E Calculation of leaf metabolic activity indices

Based on the intrinsic electrophysiological parameters and water-use indices, the following indices of relative metabolic vigor are derived.

The nutrient transfer rate (STR) combines water holding capacity and holding time, reflecting the rate of nutrient movement associated with water transport:

$$\mathrm{STR} = \frac{\mathrm{LIWHC}}{\mathrm{LIWHT}} \tag{S.54}$$

The active nutrient transport flow per unit leaf area (UAF) represents the ratio of capacitive reactance to inductive reactance, reflecting the relative contribution of surface proteins to intrinsic proteins in nutrient transport:

$$\mathrm{UAF} = \frac{\mathrm{IX}_C}{\mathrm{IX}_L} \tag{S.55}$$

The active nutrient transport capacity in leaves (NAC) is the product of STR and UAF, integrating water-mediated transport rate with membrane protein composition:

$$\mathrm{NAC} = \mathrm{STR} \times \mathrm{UAF} \tag{S.56}$$

The leaf metabolic flow (MF) is defined as the reciprocal of the product of all four intrinsic electrophysiological parameters (IR, IZ, IX_C, IX_L). This composite index reflects the overall conductance capacity of the leaf tissue:

$$\mathrm{MF} = \frac{1}{\mathrm{IR} \times \mathrm{IZ} \times \mathrm{IX}_C \times \mathrm{IX}_L} \tag{S.57}$$

The leaf metabolic rate (MR) is the product of STR and NAC, representing the integrated rate of nutrient transfer and active transport:

$$\mathrm{MR} = \mathrm{STR} \times \mathrm{NAC} \tag{S.58}$$

Finally, the relative metabolic activity (MA) is derived as the geometric mean of MF and MR, providing a comprehensive measure of cellular metabolic vigor:

$$\mathrm{MA} = (\mathrm{MF} \times \mathrm{MR})^{1/6} \tag{S.59}$$

Yuxuan Gong holds a B.S. in Biological Science and is completing her M.S. in Ecology at Jiangsu University. Her graduate research focuses on plant electrobiology and water-saving irrigation. (Email: 2531553716@qq.com)

Deke Xing holds a Ph.D. in Geochemistry, M.S. in Agricultural Bioenvironment and Energy Engineering, and B.S. in Environmental Science. His research focuses on plant electrobiology, plant stress physiological ecology, and water-saving irrigation. He has successfully applied electrobiological techniques to research in plant stress physiological ecology and water-saving irrigation. By employing electrobiological techniques, he investigated the dynamic characteristics of intracellular water utilization in various plant species under stresses. Meanwhile, he developed models that correlates electrobiological parameters with the plant's net photosynthetic rate and growth status, allowing for the precise prediction of both the net photosynthetic rate and growth rate. These models have also been applied to the precision irrigation. He serves as Associate Editor of Journal of Plant Electrobiology. (Email: xingdeke@ujs.edu.cn)

Linpu Wu holds a B.S. in Biological Science and she is currently a M.S. student at the Ecology from Jiangsu University, Zhenjiang, China. Her research focuses on plant electrobiology and water-saving irrigation. (Email: 2052450359@qq.com)

Huiwen Chen is currently pursuing a Master's degree in Ecology at Jiangsu University. Her primary research focuses on applying plant electrophysiological techniques to investigate the diurnal dynamics of intracellular water (and nutrient) in the leaves of CAM plants and C_3 plants. (Email: chw2373511052@163.com)

Junle Li holds an M.S. in Ecology from Jiangsu University and a B.S. in Horticulture from Southwest University. His research focuses on plant stress physiology, physiological ecology, and precision agriculture technology. (Email: 906629714@qq.com)

Qian Zhang holds an M.S. in Ecology from Jiangsu University. Her research focuses on the coupling of intracellular water dynamics with plasma membrane intrinsic proteins (PIPs) and tonoplast intrinsic proteins (TIPs) in tomato leaves during drought and rehydration. The study intends to provide deeper insights into the regulatory role of PIPs/TIPs in plant water relations at the cellular level and offer new perspectives for developing novel methodologies for monitoring plant water status. (Email: 2212216008@stmail.ujs.edu.cn)